Structural, morphological and optical studies of chemically developed annealed Cu doped CdS nanofilms

S. KUMAR[1], AFTAB ALAM[2], D. K. SINGH[3], S. K. SHARMA[4], S. R. KUMAR[5], S. RAJPAL[6,*]
[1] Department of Physics, Chaibasa Engineering College, chaibasa, J harkhand, 833215, India
[2]Department of Engineering Physics, Al-Kabir polytechnic, Jamshedpur, Jharkhand -831012, India
[3]Department of Physics, P.K. Roy Memorial College, Dhanbad, Jharkhand-826004, India
[4]Department of Physics, Indian Institute of Technology (IIT-ISM), Dhanbad, Jharkhand-826004, India
[5]Department of Applied Science, National Institute of Advanced Manufacturing Technology, Hatia, Ranchi-83400, India
[6]Department of Physics, Government Engineering College Munger, Bihar- 811201, India

In this work, Cu doped CdS thin films were developed by chemical bath deposition technique at 140℃ on ITO glass substrate. The film was annealed at 350℃ in air. By using XRD, FESEM, WCA, UV-VIS, and FTIR the structural, morphological, and optical characteristics of the films were examined. The samples appear to be polycrystalline based on X-ray diffraction (XRD) data, and other characteristics including crystallite size, micro strain, and dislocation density were evaluated. A FESEM analysis reveals that uniform distribution grains with spherical shapes cover the entire substrate surface. The bandgap of thin films was calculated using Tauc theory with increase of annealing temperature. Based on the results of these experiments, the potential for using Cu doped CdS films as a window layer was studied.

1. Introduction

Few decades ago, many researchers have been considerable interest on semiconductor materials because of their properties permits in large areas of technological applications like photodetectors, transistors, diodes, thermistors, solar cells, etc. Initially, silicon-based semiconductor can be used for making devices but their manufacturing cost is expensive. So, research community have been attracted towards II-VI group focusing on chalcogenides family such as cadmium sulphide, cadmium telluride, zinc oxide etc [1]. Now with standing to this, the above said materials are needed to explore for both academically and scientifically. Large-scale uses for metal chalcogenide thin films include superconducting and magnetic mateials, diamond-like films, hard coatings, microelectronic devices, infrared detectors, optical imaging, photoconductors, solar cells, memory (optical mass), solar control, sensors, and photodiodes [2]. Various researchers have focused on II-VI group of semiconducting material like Cadmium sulphide, Zinc sulphide, etc because it can be helpful for the fabrication of solar cells together with optoelectronic devices [3,4]. Cadmium sulphide (CdS) lies under the umbrella of chalcogenide family and has to be concentrated because of its wide bandgap so it can be used for LEDs, photodetectors, photovoltaic cell, transistors, gas sensors, optical filters, optoelectronic devices [5,6], photo electrochemical hydrogen formation [7], treatments of waste water [8,9], optical waveguides, nonlinear integrated optical devices [10,11]. When thin film solar cells are formed, CdS thin film can be considered as a potential candidate for the window layers. The potential of

CdS depend on the availability of significant photoconductivity, enhance transmittance and luminescence properties in the visible and infrared regions [12, 13], and uniform morphology to avoid short circuit effects. Copper (Cu) can be considered in the form of an acceptor if it is doped into CdS thin film. After doping there will be changes its behavior such as resistivity, energy bandgap, photoelectrical conversion of N to P type semiconductor [14]. Normally, Cu diffusion has been used to obtain the p-type of semiconductors. They were able to get a 6-7% efficiency by a Cu. For use in solar applications, Cu:CdS/CdS homostructure were used [15]. Thermal evaporation [16,17], MBE [21], spray pyrolysis [19], anodic oxidation [20], cathodic reduction [18], and Chemical Bath Deposition [22-26] are some of the methods that have been used to deposit Cu doped CdS thin films. Cu doped CdS films can be developed using the CBD method [27,28] since it offers many advantages over other deposition methods, including the simple technique, low price, large-area deposition, uniform & smooth gains, homogenous and creates films of high grade.

Various academicians and researchers have been developed Cu doped CdS nanocrystalline thin films over such substrates like glass/ ITO glass/ FTO glass, etc in aqueous solution by using chemical bath deposition method [29,30].

In this paper, we report the development of Cu doped CdS nanocrystalline thin films over ITO glass substrate in non-aqueous medium using Chemical bath deposition technique. The important parameters studied here are structural, surface morphological, hydrophobicity nature,

optical energy (bandgap) etc of developed Cu doped CdS thin films.

2. Experimental details

The AR grade of 0.40M cadmium acetate, 0.10M copper sulphate, 75 ml (1:2) of ethylene glycol and ethanol were taken to synthesize the electrolyte. At a temperature of 140°C, the electrolyte was agitated for 2h. By the use of a sturdy support, an ITO glass substrate was placed into the electrolyte and 0.27M thiourea were added in the solution. The colour starts with blue, changed to a light green after 8 to 10 minutes, and then kept taking on a yellowish green colour. The electrolyte was stirred continuously as it was applied to the ITO glass substrate for 20 minutes. The deposited Cu doped CdS films over ITO glass substrate exhibit good adhesion and are physically stable. The produced Cu doped CdS film was annealed in air at 350°C. Bruker AXS diffractometer model: D8 was employed to investigate the crystallographic structure of Cu doped CdS for both as deposited and annealed films at CuK wavelength 1.54Å. Using Debey-Scherrer's equation the average crystalline size of Cu doped CdS nanocrystalline films were determined. With the use of a Field Emission Scanning Electron Microscope (FESEM), model: Quanta 200F, FEI Netherland, surface morphology analyses of the films were carried out. The water contact angle measurement which is examined using a water contact angle measuring instrument (WCA, Philips) is used to assess whether the deposited films are hydrophilic or hydrophobic. The UV-VIS spectrophotometer Lambda-25 Perkin-Elmer model was used for the determination of energy band spectra. Shimadzu's IR Prestige-21 spectrometer was used to perform FTIR analysis on both films in the wave number range of 500cm^{-1} to 4000cm^{-1}.

3. Results and discussion

3.1. Structural analysis

Fig. 1 represents the XRD pattern of Cu doped CdS nanocrystalline thin films between 20-90 degrees. The diffraction prominent sharp peaks were existed at an angle of 2θ= 24.73°, 26.19°, 27.79°, 37.78° and 48.22° corresponding to the planes of (100), (002), (101), (220) and (103) for Cu doped CdS as deposited films. Peak appeared at 2θ=26.19° correspond to the hexagonal structure of the crystal (JCPDS card no 41-1049). Reflections from the ITO glass substrate are accountable for the subsequent peaks at 32.99°, 43.42°, 52.71° and 60.14° which are attributed to scattering from the (222), (110), (200) and (202) planes. When Cu doped CdS nanocrystalline thin film was annealed at 350°C, the characteristics peaks appeared at 24.84°, 26.38°, 27.78°, 36.42°, 37.72°, 48.25° and 74.34° corresponding to the planes of (100), (002), (101), (102), (220), (103) and (114).
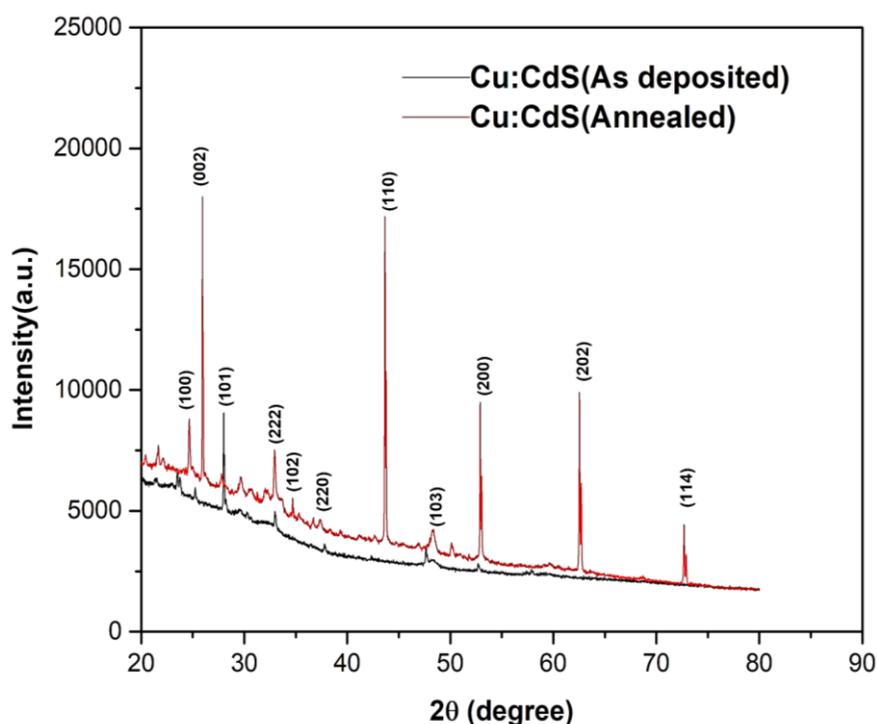
Fig. 1. XRD Spectra of As deposited and annealed Cu doped CdS thin films (color online)

After being annealed at 350°C, the appropriate peak (002) is established at a slightly higher angle with 26.38° and two new peaks appear at 36.42° and 74.34°, as shown in Fig. 1.

The crystalline size of Cu doped CdS nanocrystalline for as deposited and annealed thin films were calculated by using Scherrer's relation [31], D= 0.94λ/β Cosθ, Where, λ is the wavelength of the X-ray used (1.54Å), β is the full-width at half maxima (FWHM) of the peak which has maximum intensity, θ is the angle of diffraction. The equation below is used to compute the microstrain that generated in both films [32], Microstrain $(\mathcal{E}) = \beta Cos\theta/4$. The following formula [33] is used to evaluate the dislocation density (δ) of Cu doped CdS nanocrystalline thin films which have been deposited and annealed, Dislocation density (δ) $=1/D^2$.

The average crystalline size of as-deposited and annealed Cu doped CdS nanocrystalline thin films were calculated as 15.73 nm and 20.08 nm respectively. The increment diffusion of the absorbed species which thus led to an enhancement in the crystallinity of Cu doped CdS films is attributable increase in (002) preferred orientation after annealing [34]. The enhancement in crystallinity is clearly demonstrated by the rise in average crystalline size driven on with annealing. The recombination centre at the grain boundary is diminished of the reducing grain boundaries caused by an increase in average crystalline size [35]. Table 1 presents the calculated 2θ, FWHM, crystalline size, microstrain, and dislocation density of Cu doped CdS thin films that were deposited and then annealed.

Table 1. Average crystalline size, micro-strain and dislocation density of Cu doped CdS as deposited and annealed thin films

Compound	2θ	FWHM	crystalline Size (D)	Micro strain (Ɛ)	Dislocation density (δ)
Cu doped CdS (As deposited)	26.19	0.541	15.73 nm	$0.229×10^{-3}$	0.0040415 (nm^{-2})
Cu doped CdS (Annealed)	26.38	0.424	20.08 nm	$0.180×10^{-3}$	0.0024801 (nm^{-2})

3.2. Surface morphology studies

FESEM is a technique that has a lot of potential for studying the topography of materials and it provides crucial details about the way that particles grow and take on their shape. Fig. 2 (a) and (b) shows the morphologies of the Cu doped CdS nanocrystalline thin films in as deposited and annealed conditions. In order to study the developed and annealed films FESEM magnification is taken at 5.00KX. Surface morphology of as deposited films in Fig. 2(a) indicates that the deposited films have smooth, dense and uniform surface, which is lacking of pinholes or fractures. On the film's surface, it has been noted that there are areas where grains seem to be present both individually and in bunches. The surface of the film changes when it is annealed at 350°C. The film reveals a rough and spongy surface shape, and some big crystals formed by agglomerates can be seen, as illustrated in Fig. 2(b).
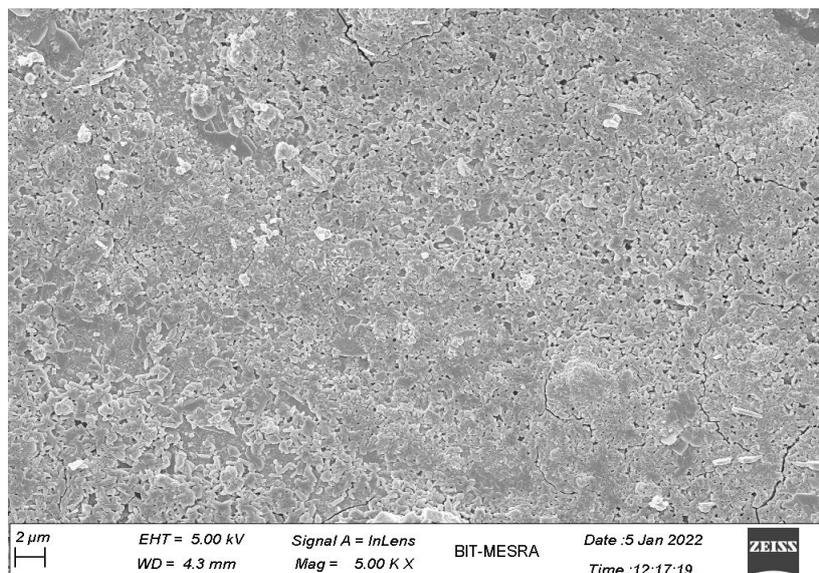
(a)
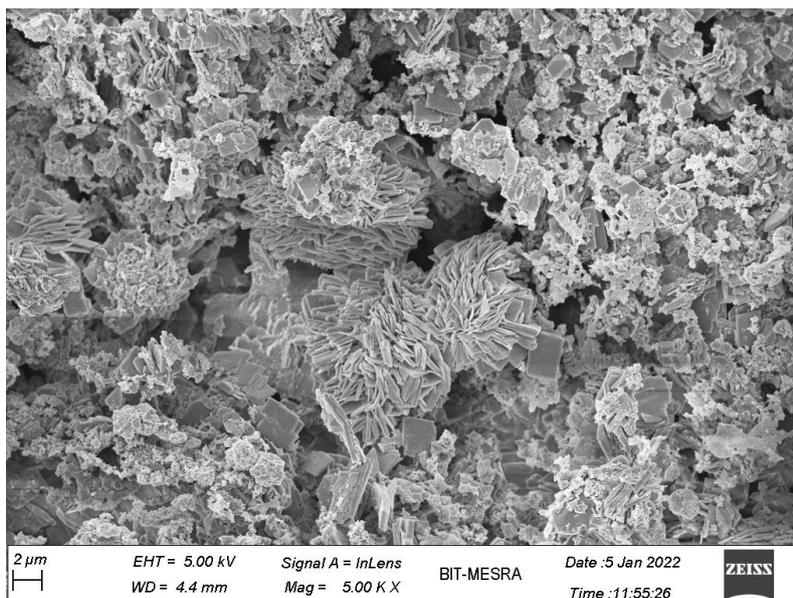
(b)

Fig. 2. FESEM images of Cu doped CdS (a) As   deposited and (b) Annealed thin films

3.3. Wettability studies

Water contact angle measurement (θ) is used in wettability studies to describe the surface's wetting nature. The important characteristics of a solid surface that determine the relationship between water droplets and its surface are hydrophobicity and hydrophilicity. When wettability is high, contact angle will be low (θ<90^0), indicating a hydrophilic surface, while when wettability is low, contact angle will be high (θ>90^0), indicating a hydrophobic surface. Fig. 3 (a) suggests that the contact angle for Cu doped CdS nanocrystalline as-deposited film should be 39.27^0, indicating that the film should be hydrophilic in nature. However, Fig. 3 (b) shows that the contact angle should be 65.56^0 for annealed film. According to this study, we conclude that wettability properties of Cu doped CdS nanocrystalline as deposited and annealed films prepared in non-aqueous medium are hydrophilic in nature.
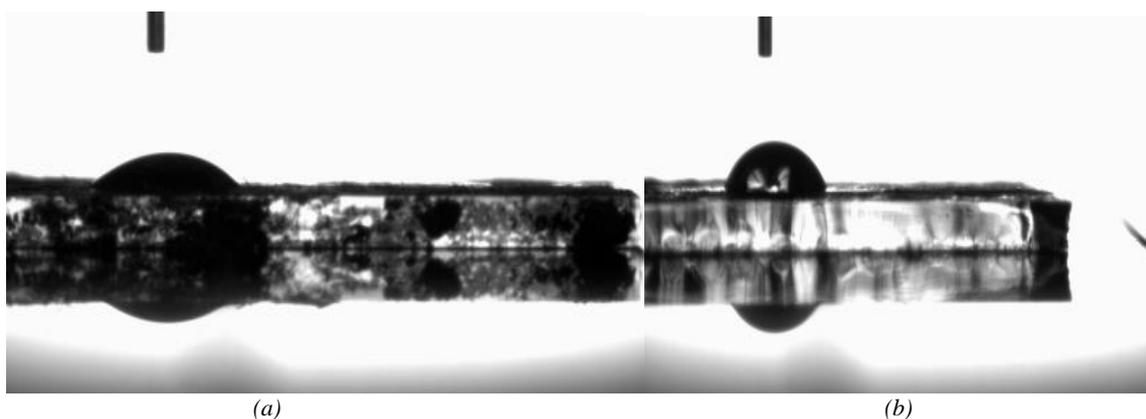
(a)   *(b)*

Fig. 3. WCA image of Cu doped CdS (a) as deposited and (b) annealed thin films (color online)

3.4. UV-VIS studies

Cu doped CdS is known to be a type of direct bandgap semiconductor. The absorption coefficient (α) on photon energy (hv) has the following relationship, using Tauc theory: $(\alpha h v)^{1/m} = A (h v - E_g)$ Where, A is a constant, E_g is the optical bandgap and m=1/2 for direct type of transition.

(a)

(b)
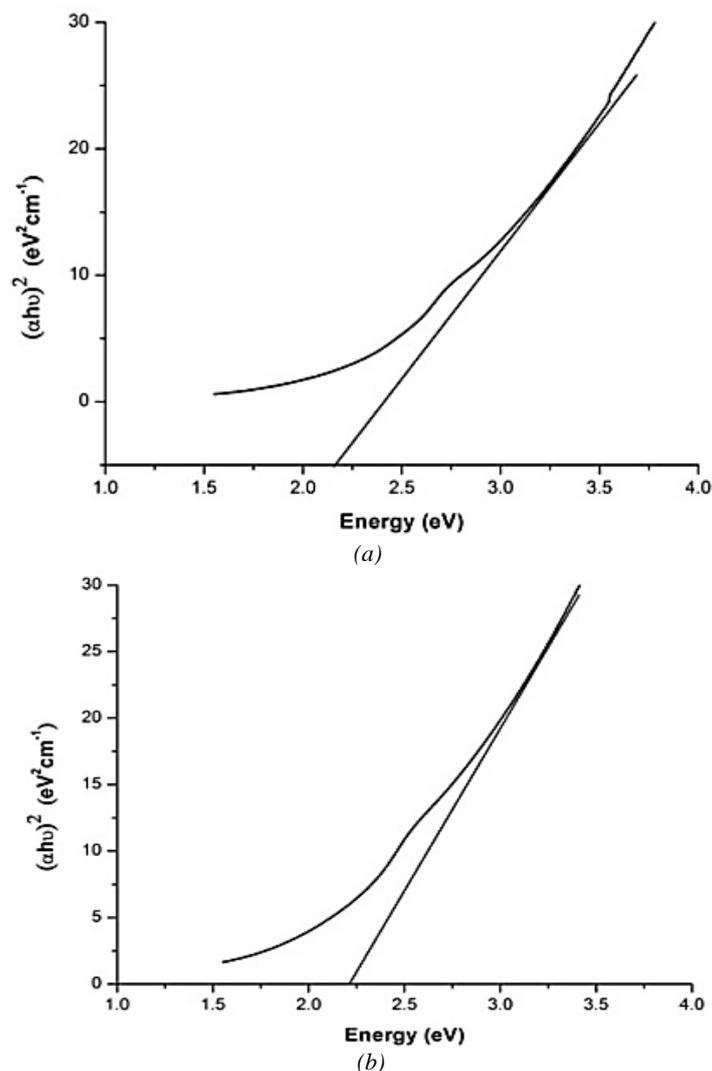
Fig. 4. $(\alpha h\nu)^2$ vs. Energy of Cu doped CdS (a) as deposited and (b) annealed thin films

The optical absorption spectra of a Cu-doped CdS nanocrystalline thin films are shown in Fig. 4 (a) and (b), which represent a plot of $(\alpha h\nu)^2$ vs. hν and the bandgap (E_g) of the material is calculated by extrapolating the curve for $(\alpha h\nu)^2$=0. The materials from the present study are of direct band gap nature and after annealing, bandgap is also found to minutely increases from 2.18 eV to 2.2 eV. Band gaps of the deposited film grow as a result of annealing, which is related to the improvement in crystallinity [36-38]. Using the relation provided by Ravindra et al. [39], the refractive index was calculated using the energy gap values.

Table 2. Relation between bandgap and refractive index

Sample	Bandgap (eV)	Refractive index (n) n= 4.08-0.62E_g
Cu:CdS As deposited	2.18	2.73
Cu:CdS Annealed	2.2	2.71

3.5. FTIR studies

FTIR is utilized to identify and classify the organic species/elements that make up the material. Figure 5 shows the FTIR analysis of Cu doped CdS nanocrystalline films grown over ITO glass substrate using the chemical bath deposition method. All peaks in the spectra of the above-mentioned films were identified during analysis using a spectrometer in the wavenumber range of 500 cm^{-1} to 4000 cm^{-1}. A peak of 3738 cm^{-1} is illustrated in Fig. 5 and is attributed to O-H stretching of water that has been absorbed on the surface of CdS films. The bending vibration of deposited film at 1625 cm^{-1} and weak bending vibration at 1516 cm^{-1} [40] also show the presence of water. Moreover, the Cd-O vibrations are important for the weak both symmetric and asymmetric absorption bands that were observed at 2806 cm^{-1} and 2900 cm^{-1} respectively. 2358cm^{-1} is accountable for the CH group's development. The SO$_2$ bond can be attributed to the peak which occurred at 1285 cm^{-1} and 1122 cm^{-1}. The C-C stretching is revealed by the absorption peak which occurs at 1516 cm^{-1} and 1408 cm^{-1}. The peak appeared at 969 cm^{-1}, and S-S-S bending is

involved for 816cm⁻¹. The peak 694cm⁻¹ is due to bending vibration of Cd-S. The peak 620cm⁻¹ is due to the Cd-S stretching vibration.
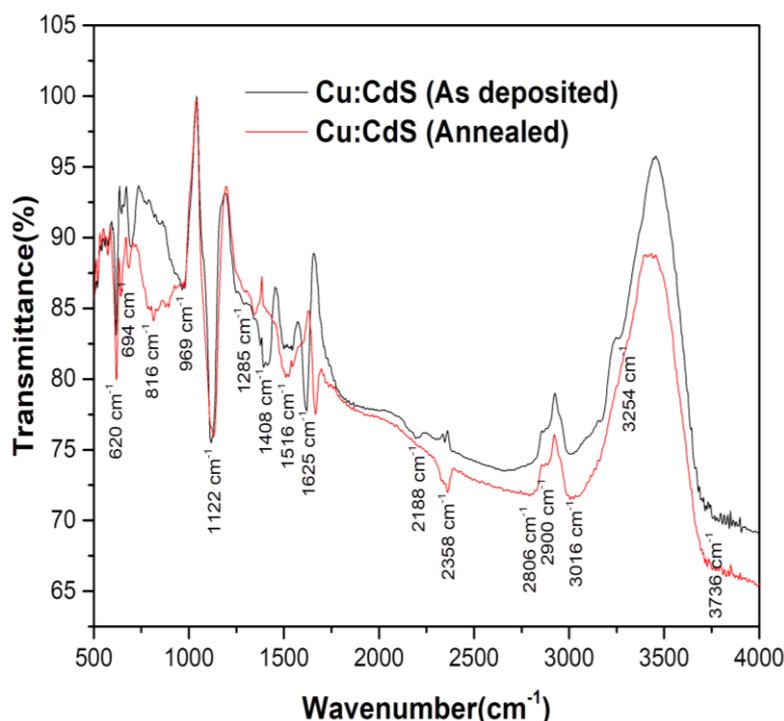
Fig. 5. FTIR Spectra of Cu doped CdS as deposited and annealed thin films (color online)

4. Conclusions

In this paper, non-aqueous medium and the CBD approach were employed to synthesize Cu doped CdS nanocrystalline films on an ITO glass substrate. CBD is a simple, cheap technique that performs well for large-area thin film depositions. XRD, FESEM, WCA, UV-VIS, and FTIR were used to analyze the films as they were deposited and annealed. Cu doped CdS nanocrystalline thin films have a hexagonal structure with a (002) plane, according to the XRD data. According to the FESEM study, the deposition is smooth and uniform and free of pinholes, pits, voids, etc. The bandgap of the deposited films is 2.2 eV and after annealing it is observed to be 2.19 eV. The deposited films are useful for optoelectronic devices and solar cells because of their larger bandgap. The stretching of -OH is observed at 3738 cm-1 in FTIR spectra. At 2358 cm⁻¹, the CH group is observable. Cu doped CdS nanocrystalline films have been found to have the suitable optical properties and energy bandgap values for photovoltaic solar cell applications.

References

[1] O. Madelung, III-V compounds. Semiconductors: Data Handbook, Springer-verlag, Berlin, Heidelberg, Germany, 71 (2004).
[2] A. K. Singh, S. Mehra, G. S. Thool, European Chemical Bulletin **2**(8), 518 (2013).
[3] Y. Gu, E. S. Kwak, J. L Lensch, J. E. Allen, T. W. Odom, L. J. Lauhon, Applied Physics Letters **87**, 043111 (2005).
[4] P. K. C. Pillai, N. Shroff, A. K. Tripathi, Journal of Physics D: Applied Physics **16**, 393 (1983).
[5] S. Prabahar, M. Dhanam, Journal of Crystal Growth **285**, 41 (2005).
[6] S. Saravanakumar, K. S. Usha, G. Vijayaprasath, J. Mat. Sci.: Mater. Electron. **34**, 3 (2023).
[7] Alka Pareek, Rekha Dom, Pramod H. Borse, International Journal of Hydrogen Energy **38**, 36 (2013).
[8] Alireza Nezamzadeh-Ejhieh, Zohreh Banan, Desalination **284**, 157 (2012).,
[9] Somayeh Azimi, Alireza Nezamzadeh-Ejhieh, Journal of Molecular Catalysis A: Chemical **408**, 152 (2015).
[10] B. G. An, Y. W. Chang, H. R. Kim, G. Lee, M. J. Kang, J. K. Park, J. C. Pyun, Sensors and Actuators B: Chemical **221**, 884 (2015).

[11] Md. Ferdous Rahman, Md. Mahabub Alam Moon, Md. Hasan Ali, Shamim Ahmmed, Samia Tabassum, Jaker Hossain, Abu Bakar Md. Ismail, Optical Materials **117**, 111136 (2021).

[12] R. Castro-Rodŕiguez, A. I. Oliva, V. Sosa, F. Caballero-Briones, J. L. Peňa, Applied Surface Science **161**, 340 (2000).

[13] S. Hemathangam, G. Thanapathy, S. Muthu Kumaran, J. Mater. Sci.: Mater. Electron. **27**, 1791 (2016).

[14] Y. Kashiwaba, K. Isojima, K. Ohta, Solar Energy Materials and Solar Cells **75**, 253 (2003).

[15] Y. Kashiwaba, T. Komatsu, M. Nishikawa, Y. Ishikawa, K. Segawa, Y. Hayasi, Thin Solid Films **408**, 43 (2002).

[16] G. B. Smith, A. Ignatiev, G. Zajac, Journal of Applied Physics **51**, 4186 (1980).

[17] K. Chidambaram, L. K. Malhotra, K. L. Chopra, Thin Solid Films **87**, 365 (1982).

[18] J. Nishino, T. Kawarada, S. Ohshio, H. Saitoh, K. Maruyama, K. Kamata, Journal of Materials Science Letters **16**, 629 (1997).

[19] W. S. Hu, Z. G. Liu, X. L. Guo, C. Lin, S. N. Zhu, D. Feng, Materials Letters **25**, 5 (1995).

[20] J. F. McCann, M. S. Kazacos, Journal of Electroanalytical Chemistry and Interfacial Electrochemistry **119**, 409 (1981).

[21] G. Hodes, J. Manassen, S. Neagu, D. Cahen, Y. Mirovsky, Thin Solid Films **90**, 433 (1982).

[22] C. Nethravathi, S. Sen, N. Ravishankar, M. Rajamathi, C. Pietzonka, B. Harbrecht, The Journal of Physical Chemistry B **109**, 11468 (2005).

[23] Md. Ferdous Rahman, Jaker Hossain, Abdul Kuddus, Samia Tabassum, Mirza H. K. Rubel, Hajime Shirai, Abu Bakar, Md. Ismail, Applied Physics A **126**, 145 (2020).

[24] S. Saravanakumar, R. Premarani, R. Chandramohan, J. Jebaraj Devadasan, J. Thirumalai, J. Mater Sci: Mater. Electron. **28**, 12092 (2017).

[25] M. F. Rahman, J. Hossain, A. B. M. Ismail, SN Appl. Sci. **2**, 1956 (2020).

[26] S. Kumar, N. S. Negi, S. C. Katyal, Pankaj Sharma, Vineet Sharma, Journal of Magnetism and Magnetic Materials **367**, 1 (2014)

[27] L. Zhou, Y. Xue, J. Li, Journal of Environmental Sciences **21**, S76 (2009).

[28] Md. Mahabub Alam Moona, Md. Ferdous Rahman, Md. Kamruzzaman, Jaker Hossain, Abu Bakar Md. Ismail, Energy Reports **7**, 1742 (2021)

[29] P. Venkatesu, K. Ravichandran, Adv. Mat. Lett. **4**(3), 202 (2013)

[30] Md. Ferdous Rahman, Jaker Hossain, Abdul Kuddus, Md. Mahabub Alam Moon, Abu Bakar Md. Ismail, SN Applied Sciences **2**, 590 (2020).

[31] S. Kumar, S. Rajpal, S. K. Sharma, D. Roy, S. R. Kumar, Chalcogenide Letters **14**, 17 (2017).

[32] Raghad Y. Mohammed, S. Abduol, Ali M. Mousa, International Letters of Chemistry, Physics and Astronomy **29**, 91 (2014).

[33] Guangxing Liang, Ping Fan, P. J. Cao, Z. H. Zheng, Materials Science Forum **743**, 915 (2013).

[34] Sanjay A. Gawali, C. H. Bhosale, Materials Chemistry and Physics **129**, 751 (2011).

[35] S. Rajpal, V. Bandyopadhyay, Journal of Nano-and Electronic Physics **5**, 03021-1 (2013).

[36] T. Premkumar, S. Saravanakumar, K. Sankaranarayanan, Applied Surface Science **257**, 1923 (2011).

[37] N. M. Ravindra, S. Auluck, V. K. Srivastava, Physica Status Solidi B **93**, K155 (1990).

[38] Mohamed Shaban, Mona Mustafa, A. M. El Sayed, Materials Science in Semiconductor Processing **56**, 329 (2016).

[39] S. Kumar, S. Rajpal, S. K. Sharma, D. Roy, S. R. Kumar, Digest Journal of Nanomaterials and Biostructures **12**, 339 (2017).

[40] P. Samarasekara, P. A. S. Madushan, Materials Science **1**, 9 (2016).

_____

*Corresponding author: sraj1162@gmail.com